

Tricarbonylmanganese(I) derivatives of [Di(pyrazolyl)(2-pyridyl)methyl]aryl scorpionates

Daniel L. Reger*, James R. Gardinier, T. Christian Grattan, Mark D. Smith

Department of Chemistry and Biochemistry, University of South Carolina, Columbia, SC 29208, USA

Received 27 August 2004; accepted 25 October 2004

Available online 29 December 2004

Abstract

The cobalt(II) chloride catalyzed Peterson rearrangement reactions between sulfinyldi-(pyrazolyl) and aryl(pyridyl)methanone derivatives yield di(pyrazolyl)(pyridyl)hetero-scorpionate ligands. Reaction of these ligands with $\text{Mn}(\text{CO})_5\text{Br}$ in the presence of a silver salt produces the monometallic complexes $\{[\kappa^3\text{-PhC}(\text{pz})_2(2\text{-py})]\text{Mn}(\text{CO})_3\}(\text{O}_3\text{SCF}_3)$ (**1a**), $\{[\kappa^3\text{-PhC}(\text{pz})_2(2\text{-py})]\text{Mn}(\text{CO})_3\}(\text{PF}_6)$ (**1b**), $\{[\kappa^3\text{-PhC}(\text{pz})_2(2\text{-py})]\text{Mn}(\text{CO})_3\}(\text{PF}_6)$ (**2**), $\{[\kappa^3\text{-}p\text{-BrC}_6\text{H}_4\text{C}(\text{pz})_2(2\text{-py})]\text{Mn}(\text{CO})_3\}(\text{PF}_6)$ (**3**), and the bimetallic complexes $[(\text{CO})_3\text{Mn}\{m\text{-C}_6\text{H}_4[\text{C}(\text{pz})_2(2\text{-py})]_2\}\text{Mn}(\text{CO})_3](\text{BF}_4)_2$ (**5a**) and $\{m\text{-C}_6\text{H}_4[\text{C}(\text{pz})_2(2\text{-py})]\text{Mn}(\text{CO})_3\}_2(\text{PF}_6)_2$ (**5b**) (pz = pyrazolyl ring, py = pyridyl ring). These octahedral manganese complexes show interesting structural diversity, with the complexes being organized in the solid state into complex supramolecular structures by an array of non-covalent forces.

© 2004 Elsevier B.V. All rights reserved.

Keywords: Manganese; Supramolecular structures; Tris(scorpionate) ligands

1. Introduction

There is substantial interest in the planned syntheses of coordination network solids for use in materials chemistry and catalysis [1]. An important feature in this field is the design of specific types of ligands that are capable of binding to metal centers in a predictable manner defined in part by the geometry of the ligand. We have been developing the syntheses of tris(pyrazolyl)methane and related ligands [2]. These ligands, especially those in which we link two or more of the tris(pyrazolyl)methane units in a single (multitopic) ligand, offer substantial structural diversity. The multiple coordination modes and ability of these ligands to support important non-covalent interactions such as weak hydrogen bonds [3], $\pi\text{-}\pi$ stacking [4], $\text{X-H}\cdots\pi$ interactions ($\text{X} = \text{O}, \text{N}, \text{C}$) [5], and interhalogen interactions

[6] is responsible for the structural diversity in their metal complexes. In our previous chemistry on multitopic ligands, we have mainly employed semi-rigid linking groups, such as in $\text{C}_6\text{H}_6\text{-}_n[\text{CH}_2\text{OCH}_2\text{C}(\text{pz})_3]_n$ ($n = 2, 3, 4, 6$) in the formation of discrete coordination complexes and coordination polymers [7]. We have also reported the syntheses of heteroscorpionate ligands based on di(pyrazolyl)(2-pyridyl)methane units, including a fixed geometry ligand, $m\text{-C}_6\text{H}_4[\text{C}(\text{pz})_2(2\text{-py})]_2$ (pz = pyrazolyl ring, py = pyridyl ring) [8]. The silver derivatives of this potentially bitopic ligand were discrete AgL_2 species that had κ^2 -bonding of only one of the two potentially tridentate $[\text{C}(\text{pz})_2(2\text{-py})]$ units rather than coordination polymers or metallacycles as originally intended and as seen in other linked scorpionate ligands. The discrete silver structure was nonetheless interesting in that it had layered arrays of metal ions held together via multiple noncovalent interactions involving the atoms of the ligand framework. The silver complex of the monotopic ligand $\text{PhC}(\text{pz})_2(2\text{-py})$ also shared these structural features [8]. In order to more

* Corresponding author. Tel.: +1 803 777 2587; fax: +1 803 777 9521.

E-mail address: reger@mail.chem.sc.edu (D.L. Reger).

fully develop the chemistry of these heteroscorpionate ligands, we report here their coordination chemistry with tricarbonylmanganese(I) cations and explore the effects of substitution along the ligand periphery and of replacing anions on the supramolecular organization of the solids.

2. Experimental

2.1. General comments

All manipulations involving air- and moisture-sensitive compounds were carried out either in the drybox under a purified N₂ atmosphere or by using standard Schlenk techniques. The solvents were commercially available, purified by conventional means, and distilled immediately prior to use. Silica gel (230–400 mesh, 40–63 μm) for chromatographic separations was purchased from Fisher Scientific. Thionyl chloride, 1-H-pyrazole (Hpz), 1-H-4-methylpyrazole, (Hpz^{4Me}), 2-benzoylpyridine, AgBF₄, AgPF₆, and Mn(CO)₅Br were purchased from Aldrich Chemicals. Anhydrous CoCl₂ was used as purchased from Strem Chemicals. The aryl(pyridyl)methanones *p*-BrC₆H₄C(O)(2-py), *m*-[(2-py)C(O)]₂-C₆H₄ [9], and *p*-(2-py)₂NC₆H₄C(O)(2-py) [10] were prepared according to the literature routes. The ligands **L1** [2] and **L5** [8] and the manganese complex {[κ³-PhC(pz)₂(2-py)]Mn(CO)₃}₂(O₃SCF₃) (**1a**) were prepared as previously described [2]. Robertson MicroLit Laboratories, Inc. (Madison, NJ) performed all elemental analyses. Samples for melting point determinations were contained in flame sealed capillaries and the reported temperatures are uncorrected. The NMR spectra were recorded by using either a Varian Gemini 300 or a Varian Mercury 400 instrument, as noted within the text. Chemical shifts were referenced to solvent resonances at δ_H 7.27 and δ_C 77.23 for CDCl₃ or at δ_H 2.05 and δ_C 29.15 for acetone-d₆. Infrared spectra were recorded for samples as CH₂Cl₂ solutions between NaCl plates by using a Nicolet 5DXB FTIR spectrometer. Mass spectrometric measurements recorded in ESI(+/-) mode were obtained on a Micromass Q-ToF spectrometer whereas those performed by using direct probe analyses were made on a VG 70S instrument.

2.2. Ligand syntheses

2.2.1. PhC(4-Me pz)₂(2-py), α,α-Bis(4-methyl-1-pyrazolyl)-α-(2-pyridyl)toluene (**L2**)

A mixture of 7.5 mmol SO(pz)₂ [from 0.35 g (15 mmol) NaH, 1.2 g (15 mmol) Hpz^{4Me}, and 0.55 ml (7.5 mmol) SOCl₂], 1.3 g (6.9 mmol) 2-benzoylpyridine, and 0.20 g (22 mol% of **1**) CoCl₂ in 20 ml THF were heated at reflux for 48 h. The resulting mixture was partitioned between 50 ml each CH₂Cl₂ and water. The sep-

arated aqueous fraction was extracted with four 50 ml portions of CH₂Cl₂. The combined organic phases were dried over MgSO₄, filtered and solvent was removed by rotary evaporation to leave a yellow oil. Chromatographic separation of the product mixture on SiO₂ with 50% Et₂O/hexanes afforded 0.61 g [27% based on PhC(O)(2-py)] of **L2** as a colorless solid from the second colorless band (*R*_f = 0.3 on TLC plate). Mp, 113–115 °C. Anal. Calcd. (Obs.) for **L2** · 1/2H₂O C₁₈H₁₆N₅O: C, 70.98 (70.86) H, 5.96 (5.55); N, 20.69 (20.79). ¹H NMR (400 MHz, CDCl₃) 8.71 (d, *J* = 4 Hz, 1H, H₆-py), 7.71 (ddd, *J* = 8, 8, 2 Hz, 1H, H₄-py), 7.49 (s, 2H, H₃-pz), 7.38–7.34 (m, 3H, Ph and py), 7.31–7.29 (m, 3H, Ph and H₅-pz), 7.24–7.21 (m, 3H, Ph and py), 2.06 (s, 6H, -CH₃). ¹³C NMR (101.62 MHz, CDCl₃) 159.0 (C₂-py), 148.8 (C₆-py), 141.4 (C₃-pz), 139.8 (C_{ipso}-Ph), 137.1 (C₄-py), 131.0 (C₅-pz), 129.4 (*o*-Ph) 129.2 (*p*-Ph), 128.2 (*m*-Ph), 124.3 (C₃-py), 123.6 (C₅-py), 116.2 (C₄-pz), 86.9 (C_α), 9.2 (CH₃). Direct probe MS *m/z* (Rel. Int.%) [assgn]: 330(49) [M]⁺, 248(100) [M-H(4-Me)pz]⁺.

2.2.2. *p*-BrC₆H₄C(pz)₂(2-py), *p*-bromo-α,α-di(pyrazolyl)-α-(2-pyridyl)toluene (**L3**)

A mixture of 6.58 mmol SO(pz)₂ [from 0.320 g (13.3 mmol) NaH, 0.905 g (13.3 mmol) Hpz, and 0.48 ml (6.58 mmol) SOCl₂], 1.71 g (6.52 mmol) *p*-BrC₆H₄C(O)(2-py), and 0.150 g (18 mol%) CoCl₂ in 50 ml THF were heated at reflux for 48 h. After aqueous work-up and extraction of organics as described for **L2** above, chromatographic separation of the product mixture on SiO₂ with 50% Et₂O/hexanes afforded unreacted *p*-BrC₆H₄C(O)(2-py) from the first (photosensitive, turns blue then brown on exposure to 254 nm light) band (TLC, *R*_f = 0.75) and then 1.08 g (45%) of **L3** as a colorless solid from the second colorless band (TLC, *R*_f = 0.4). Mp, 111–112 °C. ¹H NMR (400 MHz, CDCl₃) 8.70 (d, *J* = 5 Hz, 1H, H₆-py), 7.74 (ddd, *J* = 8, 8, 2 Hz, 1H, H₄-py), 7.69 (d, *J* = 1 Hz, 2H, H₃-pz), 7.50 (part of AA'BB', 2H, aryl) 7.48 (d, *J* = 3 Hz, 2H, H₅-pz), 7.33 (ddd, *J* = 8, 5, 1 Hz, 1H, H₅-py), 7.17 (d, *J* = 8 Hz, 1H, H₃-py), 7.13 (part of AA'BB', 2H, aryl), 6.34 (dd, *J* = 3, 1 Hz, 2H, H₄-pz). ¹³C NMR (101.62 MHz, CDCl₃) 158.2 (C₂-py), 148.9 (C₆-py), 140.9 (C₃-pz), 138.7 (C_{ipso}-Ph), 137.1 (C₄-py), 132.5 (C₅-pz), 131.3, (Ph), 131.2 (Ph), 124.4 (C₃-py), 124.0 (C_{ipso} Ph), 123.9 (C₅-py), 106.1 (C₄-pz), 86.9 (C_α). Direct Probe MS *m/z* (Rel. Int.%) [assgn]: 379 (49) [M]⁺, 313 (100) [M-pz]⁺ 301 (75) [M-Br]. HRMS Direct probe Calcd. (Obs.) for C₁₈H₁₄BrN₅: 379.0433 (379.0441).

2.2.3. *p*-[(2-py)₂N](C₆H₄)[C(pz)₂(2-py)] (**L4**)

A mixture of 0.33 g (0.94 mmol) *p*-(2-py)₂NC₆H₄-C(O)(2-py) and 1.5 mmol SO(pz)₂ [from 0.20 g (2.9 mmol) Hpz, 0.070 g (2.9 mmol) NaH, and 0.11 ml (0.18 g, 1.5 mmol) SOCl₂] in 25 ml THF was heated at

reflux for 3 d. The resulting mixture was partitioned between 50 ml each CH₂Cl₂ and water. The separated aqueous fraction was extracted with four 50 ml portions of CH₂Cl₂. The combined organic phases were dried over MgSO₄, filtered, and solvent was removed by rotary evaporation to leave a yellow oily residue. The yellow oily residue was adsorbed onto silica gel and loaded onto a silica gel column. Elution with ethyl acetate afforded unreacted *p*-(2-py)₂N₆H₄C(O)(2-py) in the first pale yellow band (TLC, *R*_f = 0.5). When the desired product began eluting (TLC, *R*_f = 0.3) a gradient of pure ethyl acetate to 1:1 ethyl acetate/acetone was used to facilitate the removal of the product from the column. Evaporation of solvents gave 0.176 g (40%) of **L4**. Mp, 176–179 °C. ¹H NMR (400 MHz, CDCl₃) 8.69 (d, *J* = 4 Hz, 1H, H₆-Cpy), 8.33 (dd, *J* = 5, 1 Hz, 2H, Npy), 7.74 (ddd, *J* = 8, 8, 2 Hz, 1H, H₄-Cpy), 7.69 (d, *J* = 1 Hz, 2H, H₃-pz), 7.58 (ddd, *J* = 8, 8, 2 Hz, 2H, H₄-Npy), 7.55 (d, *J* = 2 Hz, 2H, H₅-pz), 7.32 (ddd, *J* = 8, 5, 1 Hz, 1H, H₅-Cpy), 7.24 (d, *J* = 8 Hz, 1H, H₃-Cpy), 7.22 (part of AA'BB', 2H, aryl) 7.14 (part of AA'BB', 2H, aryl), 7.04 (d, *J* = 8 Hz, 2H, H₃-Npy), 6.97 (ddd, *J* = 7, 5, 1 Hz, 2H, H₅-Npy), 6.34 (dd, *J* = 2, 1 Hz, 2H, H₄-pz). ¹³C NMR (101.62 MHz, CDCl₃) 158.7 (C₂-Cpy), 158.1 (C₂-Npy), 148.9 (C₆-Npy), 148.8 (C₆-Cpy), 145.8 (C₇-Ph), 140.8 (C₃-pz), 137.9, 137.1 (C₄-Cpy), 135.6 (C₇-Ph), 132.6 (C₅-pz), 130.8 (Ph), 125.4 (Ph), 124.2 (C₃-Cpy), 123.8 (C₅-Cpy), 118.9 (C₃-Npy), 117.9 (C₅-Cpy), 105.8 (C₄-pz), 86.9 (C_α). Direct probe MS *m/z* (Rel. Int.%) [assign]: 470 (90) [M]⁺, 43 (100) [M-Hpz]⁺. HRMS ESI(+) Calcd. (Obs.) for C₂₈H₂₃N₈, [M + H]: 471.2046 (471.2056).

2.3. Tricarbonylmanganese complexes

2.3.1. {[κ³-PhC(pz)₂(2-py)]Mn(CO)₃}(PF₆) (**1b**)

Under a nitrogen atmosphere, a mixture of 0.196 g (0.713 mmol) Mn(CO)₅Br, 0.181 g (0.716 mmol) AgPF₆ in 10 ml acetone was heated at refluxing the the dark for 1.5 h. A yellow solution was separated from the precipitate of AgBr and was transferred by cannula filtration to a second solution containing 0.216 g (0.714 mmol) PhC(pz)₂(2-py) in 10 ml. The AgBr was washed with two 5 ml portions of acetone and these washings were also transferred to the solution containing the ligand. The resulting red-orange solution was heated at reflux for 2 h, until gas evolution ceased (monitored with an external bubbler), and then solvent was removed by vacuum distillation to leave a red orange residue. This residue was washed with two 10 ml portions of diethyl ether and dried under vacuum to leave 0.398 g (95%) of **1b**. Mp, 215 °C dec. to green solid with effervescence. Anal. Calcd. (Obs.) for C₂₁H₁₅N₅F₆O₃PMn: C, 11.97 (11.60); H, 2.58 (2.90); N, 11.97 (11.60). IR (cm⁻¹): ν_{co} 2049, 1956. ¹H NMR (500 MHz, acetone-d₆, 50 °C) 9.46 (d, *J* = 5 Hz, 1H, H₆-py), 8.67 (s, 2H, H₃-pz),

8.26 (m, 3H, aryl and H₄-py), 8.04 (d, *J* = 8 Hz, 1H, H₅-py), 7.95–7.88 (m, 5H, Ph), 7.78 (ps t, 1H, H₃-py), 6.70 (s, 2H, H₄-pz). ¹³C NMR (125.8 MHz, acetone-d₆, -20 °C) 221.0 (CO), 220.1 (CO), 157.3 (C₆-py), 156.3 (C₂-py), 149.6, 141.9, 137.8, 133.3 (Ph), 133.3, 132.6 (Ph), 129.8, 127.9, 126.8, 109.7 (C₄-pz), 83.6 (C_α).

2.3.2. {[κ³-PhC(^{4-Me}pz)₂(2-py)]Mn(CO)₃}(PF₆) (**2**)

A mixture of 0.167 g (0.607 mmol) Mn(CO)₅Br, 0.154 g (0.609 mmol) AgPF₆ in 10 ml acetone was heated at reflux in the dark for 1 h. A yellow solution was separated from the precipitate of AgBr and was transferred by cannula filtration to a second solution containing 0.216 g (0.714 mmol) PhC(^{4-Me}pz)₂(2-py) in 10 ml. The AgBr was washed with two 5 ml portions of acetone and these washings were also transferred to the solution containing the ligand. The resulting yellow-orange solution was stirred at room temperature 12 h, and then was heated at reflux for 2 h. Solvent was removed by vacuum distillation to leave an orange residue. This residue was washed with two 10 ml portions of diethyl ether and dried under vacuum to leave 0.335 g (90%) of **2** as a hygroscopic yellow solid. Mp, 235 °C dec. to green solid with effervescence. Anal. Calcd. (Obs.) for C₂₃H₂₁N₅F₆O₄PMn, **2** · H₂O: C, 43.69 (43.93); H, 3.03 (3.03), N, 11.08 (11.21). For a sample dried in 160 °C oven for 6 h and sealed while hot, Anal. Calcd. (Obs.) for C₂₃H₁₉N₅F₆O₃PMn: C, 44.97 (44.27); H, 3.12 (3.11), N, 11.40(11.14). IR (cm⁻¹): ν_{co} 2047, 1954. ¹H NMR (400 MHz, acetone-d₆, 23 °C) broad resonances 9.46, 8.53, 8.23, 7.89, 7.78, 7.70, 2.06. ¹³C NMR (101.62 MHz, acetone-d₆, 23 °C) 157.3, 149.7, 141.9, 136.1, 133.3, 132.6, 130.7, 127.8, 126.7, 120.2, 8.6. ¹H NMR (500 MHz, acetone-d₆, 55 °C) 9.43 (1H, H₆-py), 8.47 (2H), 8.21 (3H), 7.92 (2H), 7.87 (2H), 7.77 (1H), 7.69 (2H), 2.06 (6H). ¹³C NMR (101.62 MHz, acetone-d₆, -20 °C) 221.0 (CO), 220.1 (CO), 157.2 (C₆-py), 156.2 (C₂-py), 149.4 (C₃-pz), 141.7 (C₄-py), 135.9 (Ph), 133.0 (C₃-py), 132.4 (Ph), 130.5 (Ph), 129.7 (Ph), 127.6 (C₅-py), 126.5 (Ph), 119.9 (C₄-pz), 83.2 (C_α), 8.5 (CH₃). HRMS-ESI(+) (*m/z*): [M]⁺ calcd for C₂₃H₁₉N₅O₃Mn, 468.0868; found, 468.0871.

2.3.3. {[κ³-*p*-BrC₆H₄C(pz)₂(2-py)]Mn(CO)₃}(PF₆) (**3**)

A mixture of 0.205 g (0.811 mmol) AgPF₆ and 0.223 g (0.811 mmol) Mn(CO)₅Br were heated at reflux in the dark under nitrogen for 1 h, the yellow solution was transferred by cannula filtration to a solution containing 0.308 g (0.810 mmol) of *p*-BrC₆H₄C(pz)₂(2-py), **L3**. The acetone insoluble solid of AgBr was washed with 10 ml acetone and the washings were also transferred to the solution containing the ligand. The resulting red-orange solution was heated at reflux for 4 h and then solvent was removed by vacuum distillation. The residue was washed with two 10 ml portions of Et₂O and the

resulting yellow solid was dried under vacuum to give 0.510 g (90%) of **3** as a diethylether solvate, $3 \cdot 1/2\text{Et}_2\text{O}$. Mp, 215 °C dec to green solid, 250 °C black liquid. Anal. Calcd. (Obs.) for $\text{C}_{23}\text{H}_{19}\text{BrF}_6\text{N}_5\text{O}_{3.5}\text{PMn}$: C, 39.39 (38.92); H, 2.79 (2.76); N, 9.70 (9.86). IR (cm^{-1}): ν_{CO} 2049, 1956. ^1H NMR (400 MHz, acetone- d_6 , 23 °C) 9.48 (br s, 1H, $\text{H}_6\text{-py}$), 8.73 (s, 2H, $\text{H}_3\text{-pz}$), 8.25 (m, 3H, aryl and $\text{H}_4\text{-py}$), 8.08 (br m, 3H, $\text{H}_5\text{-py}$), 7.9 (m, 2H, Ph), 7.80 (br s, 1H, $\text{H}_3\text{-py}$), 6.73 (br s, 2H, $\text{H}_4\text{-pz}$), 3.40 (q, $J = 7$ Hz, 2H, $\text{Et}_2\text{O-CH}_2$), 1.11 (t, $J = 7$ Hz, 3H, $\text{Et}_2\text{O-CH}_3$). ^{13}C NMR (100.6 MHz, acetone- d_6 , -20 °C) CO not obs., 157.4 ($\text{C}_6\text{-py}$), 156.0 ($\text{C}_2\text{-py}$), 149.7, 142.0, 137.9, 134.6, 133.9, 129.2, 127.9, 127.6, 126.9, 110.0 ($\text{C}_4\text{-pz}$), 83.6 (C_α). ^1H NMR (500 MHz, acetone- d_6 , 50 °C) 9.46 (d, $J = 5$ Hz, 1H, $\text{H}_6\text{-py}$), 8.67 (s, 2H, $\text{H}_3\text{-pz}$), 8.26 (m, 3H, aryl and $\text{H}_4\text{-py}$), 8.04 (d, $J = 8$ Hz, 1H, $\text{H}_5\text{-py}$), 7.95–7.88 (m, 5H, Ph), 7.78 (ps t, 1H, $\text{H}_3\text{-py}$), 6.70 (s, 2H, $\text{H}_4\text{-pz}$). ^{13}C NMR (125.8 MHz, acetone- d_6 , -20 °C) 221.0 (CO), 220.0 (CO), 157.3 ($\text{C}_6\text{-py}$), 155.7 ($\text{C}_2\text{-py}$), 149.4, 141.8, 137.8, 134.5, 133.6, 129.0, 127.7, 127.4, 126.7, 109.7 ($\text{C}_4\text{-pz}$), 83.2 (C_α).

2.3.4. $[(\text{CO})_3\text{Mn}\{m\text{-C}_6\text{H}_4[\text{C}(\text{pz})_2(2\text{-py})]_2\}\text{-Mn}(\text{CO})_3](\text{BF}_4)_2$ (**5a**)

A mixture of 0.074 g (0.27 mmol) $\text{Mn}(\text{CO})_5\text{Br}$ and 0.053 g (0.27 mmol) AgBF_4 in 20 ml acetone was heated at reflux 3 h under nitrogen and then the yellow solution was transferred by cannula filtration (to remove AgBr) to a nitrogen-purged solution containing 0.071 g (0.14 mmol) $m\text{-C}_6\text{H}_4[\text{C}(\text{pz})_2(2\text{-py})]_2$ in 10 ml acetone. The AgBr was washed with two 5 ml portions of acetone to ensure quantitative transfer of manganese reagent to the acetone solution of the ligand. The resulting yellow solution was heated at reflux 14 h, solvent was removed by vacuum distillation, and the resulting yellow solid was washed with two 10 ml portions of Et_2O and dried under vacuum to leave 0.12 g (89%) of the desired compound as a hygroscopic yellow solid. Mp, 150–160 °C dec. with effervescence; 210 °C green. Anal. Calcd. (Obs.) for $\text{C}_{36}\text{H}_{28}\text{N}_{10}\text{B}_2\text{F}_8\text{O}_8\text{Mn}_2$, $5\mathbf{a} \cdot 3\text{H}_2\text{O}$: C, 41.98 (42.07); H, 2.94 (2.42); 13.60 (13.50). IR (cm^{-1}): ν_{CO} 2049, 1955. HRMS-ESI(+) (m/z): $[\text{M} + \text{BF}_4]^+$ calcd for $\text{C}_{23}\text{H}_{19}\text{N}_5\text{O}_3\text{Mn}$, 468.0868; found, 468.0861. Crystals suitable for single crystal X-ray structural studies were grown by vapor diffusion of Et_2O into a nitromethane solution of the complex.

2.3.5. $\{m\text{-C}_6\text{H}_4[\text{C}(\text{pz})_2(2\text{-py})\text{Mn}(\text{CO})_3]_2\}(\text{PF}_6)_2$ (**5b**)

A mixture of 0.071 g (0.26 mmol) $\text{Mn}(\text{CO})_5\text{Br}$ and 0.066 g (0.27 mmol) AgPF_6 in 20 ml acetone was heated at reflux for 2 h, then the canary yellow solution was transferred by cannula filtration to a solution of 0.068 g (0.13 mmol) **L5** in 10 ml acetone. The precipitate of AgBr from the first flask was washed with two 5 ml portions of diethyl ether and these were also transferred to

the ligand solution. The resulting red-orange solution was heated at reflux for 4 h and the solvent was removed by vacuum distillation. The orange solid was washed with several portions of diethyl ether and was dried under vacuum to leave 0.13 g (92%) of **5b** as a yellow-orange solid. IR(CH_2Cl_2) ν_{CO} 2048, 1958. ^1H NMR (300 MHz, acetone- d_6) all br s: δ_{H} 9.46, 9.10, 8.95, 8.76, 8.23, 7.77, 6.75 ($\text{H}_4\text{-pz}$). HRMS-ESI(+) (m/z): $[\text{M} + \text{PF}_6]^+$ calcd for $\text{C}_{36}\text{H}_{24}\text{F}_6\text{N}_{10}\text{O}_6\text{PMn}_2$, 947.0283; found, 947.0271.

2.3.6. Attempted preparation of $\{m\text{-}[(2\text{-py})(\text{pz})_2\text{C}]/(\text{C}_6\text{H}_4)[\text{C}(\text{pz})_2(2\text{-py})\text{Mn}(\text{CO})_3]\}(\text{PF}_6)$ (**5c**)

A mixture of 0.036 g (0.13 mmol) $\text{Mn}(\text{CO})_5\text{Br}$, 0.033 g (0.13 mmol) AgPF_6 , and 0.069 g (0.13 mmol) **L5** was reacted under the conditions described above for the preparation of **5b**. In this case, 0.085 g of a light orange solid was obtained which was identified as a 50% mixture of the desired compound and **5b** by elemental analyses and its ESI(+) mass spectrum. Anal. Calcd. (Obs.) for 50% mixture of **5c** and **5b**: C, 44.30 (44.28); H, 2.60 (3.03); N, 15.07 (14.78). ^1H NMR (400 MHz, acetone- d_6) all br s: δ_{H} 9.49 ($\text{H}_6\text{-py}$), 9.02, 8.75 (sh), 8.73 ($\text{H}_3\text{-pz}$), 8.55, 8.32, 8.20, 8.12, 7.80 ($\text{H}_3\text{-py}$), 7.70, 7.60, 7.46, 7.30, 6.76 ($\text{H}_4\text{-pz}$), 6.52 ($\text{H}_4\text{-pz}$). HRMS-ESI(+) (m/z): $[(\text{L5})\text{Mn}(\text{CO})_3]^+$ calcd for $\text{C}_{33}\text{H}_{24}\text{MnN}_{10}\text{O}_3$, 663.1411; found, 663.1413; $\{[\text{Mn}(\text{CO})_3]_2(\mu\text{-L5}) + \text{PF}_6\}^+$ calcd for $\text{C}_{36}\text{H}_{24}\text{F}_6\text{Mn}_2\text{N}_{10}\text{O}_6\text{P}$, 947.0283; found, 947.0250.

2.4. Crystallography

A yellow blocklike crystal of $\{[\text{PhC}(\text{pz})_2(2\text{-py})]\text{Mn}(\text{CO})_3\}(\text{O}_3\text{SCF}_3)$ **1a**, a yellow plate of $\{[\text{PhC}(\text{pz})_2(2\text{-py})]\text{Mn}(\text{CO})_3\}(\text{PF}_6) \cdot \text{CH}_2\text{Cl}_2$ **1b** $\cdot \text{CH}_2\text{Cl}_2$, yellow blocks of $\{[\text{PhC}(\text{pz})_2(2\text{-py})]\text{Mn}(\text{CO})_3\}(\text{PF}_6)$, **2**, and $\{m\text{-C}_6\text{H}_4[\text{C}(\text{pz})_2(2\text{-py})\text{Mn}(\text{CO})_3]_2\}(\text{BF}_4)_2 \cdot 2\text{CH}_3\text{NO}_2$, **5a** $\cdot 2\text{CH}_3\text{NO}_2$, were each mounted onto the end of thin glass fibers using inert oil. X-ray intensity data covering at least >90% of the full sphere of reciprocal space were measured at 190(1) K for **1a** and **1b** $\cdot \text{CH}_2\text{Cl}_2$, at 100(1) K for **2**, and at 150(1) K for **5a** $\cdot 2\text{CH}_3\text{NO}_2$ on a Bruker SMART APEX CCD-based diffractometer system (Mo $\text{K}\alpha$ radiation, $\lambda = 0.71073$ Å) [11]. The raw data frames were integrated with SAINT+ [11], which also applied corrections for Lorentz and polarization effects. The final unit cell parameters, see Table 1, for **1a**, **1b** $\cdot \text{CH}_2\text{Cl}_2$, **2**, and **5a** $\cdot 2\text{CH}_3\text{NO}_2$ are based on the least-squares refinement of 6294, 8578, 6647, and 8893 reflections, with $I > 5(\sigma)I$ from each respective data set. Analysis of the data showed negligible crystal decay during data collection. An empirical absorption correction based on the multiple measurement of equivalent reflections was applied to the **1a**, **1b** $\cdot \text{CH}_2\text{Cl}_2$ and **2** data sets with the program SADABS [11]. No absorption correction was applied to the **5a** $\cdot 2\text{CH}_3\text{NO}_2$ data set. The struc-

Table 1

Experimental and Crystal Data for $\{[\text{PhC}(\text{pz})_2(2\text{-py})]\text{Mn}(\text{CO})_3\}(\text{SO}_3\text{CF}_3)$ (**1a**), $\{[\text{PhC}(\text{pz})_2(2\text{-py})]\text{Mn}(\text{CO})_3\}(\text{PF}_6) \cdot \text{CH}_2\text{Cl}_2$ (**1b** · CH_2Cl_2), $\{[\text{PhC}(\text{pz})_2(2\text{-py})]\text{Mn}(\text{CO})_3\}(\text{PF}_6)$ (**2**), and $\{m\text{-C}_6\text{H}_4[\text{C}(\text{pz})_2(2\text{-py})]\text{Mn}(\text{CO})_3\}_2(\text{BF}_4)_2 \cdot 2\text{CH}_3\text{NO}_2$, (**5a** · $2\text{CH}_3\text{NO}_2$)

	Compound 1a	Compound 1b · CH_2Cl_2	Compound 2	Compound 5a · $2\text{CH}_3\text{NO}_2$
Formula	$\text{C}_{22}\text{H}_{15}\text{F}_3\text{MnN}_5\text{O}_6\text{S}$	$\text{C}_{22}\text{H}_{17}\text{Cl}_2\text{F}_6\text{MnN}_5\text{O}_3\text{P}$	$\text{C}_{23}\text{H}_{19}\text{F}_6\text{MnN}_5\text{O}_3\text{P}$	$\text{C}_{38}\text{H}_{30}\text{B}_2\text{F}_8\text{Mn}_2\text{N}_{12}\text{O}_{10}$
Molecular weight	589.39	670.22	613.34	1098.24
Temperature (K)	190(1)	190(1)	100(1)	150(1)
Crystal system	Triclinic	Hexagonal	Orthorhombic	Triclinic
Space group	P-1	$\text{P6}_3\text{cm}$	$\text{P2}_1\text{2}_1\text{2}_1$	P-1
<i>a</i> (Å)	10.1816(6)	17.8784(9)	10.2687(6)	11.0510(5)
<i>b</i> (Å)	12.0181(8)	17.8784(9)	12.8750(8)	11.5200(5)
<i>c</i> (Å)	12.0228(8)	14.9881(11)	19.3494(12)	19.0625(8)
α (°)	112.5270(10)°	90	90	81.7710(10)
β (°)	106.8640(10)°	90	90	84.8290(10)
γ (°)	104.7070(10)	120	90	69.5560(10)
<i>V</i> (Å ³)	1184.41(13)	4148.9(4)	2558.2(3)	2248.42(17)
<i>Z</i>	2	6	4	2
ρ_{calc} (g/cm ³)	1.653	1.609	1.593	1.622
μ (mm ⁻¹)	0.720	0.803	0.658	0.665
θ range (°)	2.01 to 25.03	2.28 to 26.41	1.90 to 26.39	1.90 to 25.05
Index range	$-12 \leq h \leq 12$ $-14 \leq k \leq 14$ $-14 \leq l \leq 14$	$-22 \leq h \leq 22$ $-22 \leq k \leq 20$ $-18 \leq l \leq 18$	$-12 \leq h \leq 12$ $-16 \leq k \leq 16$ $-24 \leq l \leq 22$	$-13 \leq h \leq 13$ $-13 \leq k \leq 13$ $-22 \leq l \leq 22$
Total (Indep.) Rfines	9857(4186)	22469(2993)	18798(5234)	18539(7950)
Final <i>R</i> indices [<i>I</i> > 2σ(<i>I</i>)]	<i>R</i> ₁ = 0.0598	<i>R</i> ₁ = 0.0584	<i>R</i> ₁ = 0.0441	<i>R</i> ₁ = 0.0464
<i>R</i> indices (all data)	<i>R</i> ₁ = 0.0704	<i>R</i> ₁ = 0.0668	<i>R</i> ₁ = 0.0488	<i>R</i> ₁ = 0.0636
	<i>wR</i> ₂ = 0.1655	<i>wR</i> ₂ = 0.1526	<i>wR</i> ₂ = 0.1125	<i>wR</i> ₂ = 0.1165
Largest differential Peak/hole (e/Å ³)	1.354/−0.540	0.640/−0.489	0.818/−0.342	0.398/−0.292

tures were solved by a combination of direct methods and difference Fourier syntheses, and refined by full-matrix least-squares against F^2 , using the SHELXTL software package [12]. Except where noted below in the refinement of **5a** · $2\text{CH}_3\text{NO}_2$, all non-hydrogen atoms were refined with anisotropic displacement parameters. Hydrogen atoms were placed in geometrically idealized positions and refined as standard riding atoms. Further notes regarding the structure solution and refinement for each compound can be found below.

$\{[\text{PhC}(\text{pz})_2(2\text{-py})]\text{Mn}(\text{CO})_3\}(\text{SO}_3\text{CF}_3)$, **1a**, crystallizes in the triclinic system in the space group P-1. All atoms reside on positions of general crystallographic symmetry. Disorder in the $\text{PhC}(\text{pz})_2(2\text{-py})$ ligand was observed, in the form of two of the ligating rings appearing to be a mixture of pyrazolyl/pyridyl groups. Initially the group site occupation factors for the two affected pyrazolyl/pyridyl groups were allowed to refine, constrained to sum to unity; near the end of the refinement the sofs were fixed at 0.60/0.40 (pyrazolyl/pyridyl, ring 2) and 0.40/0.60 (pyrazolyl/pyridyl, ring 3). A total of 76 restraints (SHELX FLAT, SADI and SAME) were employed to assist in the refinement of the disordered atoms.

Systematic absences in the intensity data for **1b** · CH_2Cl_2 , were consistent with the space group $\text{P6}_3\text{cm}$, clearly showing the presence of a 6_3 screw axis and a *c*-glide plane. The $\{[\text{PhC}(\text{pz})_2(2\text{-py})]\text{Mn}(\text{CO})_3\}^+$ cation is located on a mirror plane. The Mn atom, one carbonyl group (C41–O41) and the pyridine ring of

the ligand are located in the mirror plane. The mirror plane bisects the phenyl ring. The remaining pyrazolyl ring and carbonyl group atoms are located on general positions. As evident in Fig. 3, the displacement ellipsoids of pyridyl ring atoms C23 and C24, and of pyrazolyl ring atom C12 are slightly inflated compared to neighboring atoms. This indicates a slight py/pz ring disorder analogous to that observed in **1a**. However, the disorder fractions were too small to be modeled successfully (ca. <10%). Two independent PF_6^- anions are present in the asymmetric unit, both of which are disordered over special positions. The P(1) F_6^- anion occupies a position of local site symmetry C_{3v} . Four independent F atoms generate a total of 14 F positions around P1. The site occupation factors for these were allowed to refine freely until reasonable, stable values were obtained, and then they were fixed. The P(2) F_6^- anion sits on a threefold axis; the disorder of the F atoms was treated in a similar fashion as P(1). Near the end of the refinement a slight manual adjustment of the F site occupation factors was necessary to satisfy charge balance. A CH_2Cl_2 molecule of crystallization which is disordered across a mirror plane is also present in the asymmetric unit. A total of 17 geometric restraints (SHELX SADI) were used to assist in modeling the PF_6^- and CH_2Cl_2 disorder. At convergence, the absolute structure (Flack) parameter was $-0.04(4)$, indicating the correct orientation of the polar axis and the lack of racemic twinning.

Systematic absences in the intensity data of **2** were uniquely consistent with the chiral space group

P2₁2₁2₁. One {[PhC(4-Me-pz)₂(2-py)]Mn(CO)₃}⁺ and one PF₆⁻ anion, both well-ordered, are present in the asymmetric unit. At convergence, the absolute structure (Flack) parameter was 0.04(2), indicating the correct absolute structure.

Compound **5a** · 2CH₃NO₂ crystallizes in the triclinic system in the P-1 space group. All atoms reside on positions of general crystallographic symmetry. One [(CO)₃Mn(μ-*m*-L5)Mn(CO)₃]²⁺ cation, two BF₄⁻ anions and two nitromethane molecules of crystallization are present on the asymmetric unit. Extensive disorder of the {μ-*m*-C₆H₄[C(pz)₂(py)]₂} ligand and the BF₄⁻ counterions was encountered; the two included nitromethane molecules behaved normally. The disorder of the ligand takes the form of rotation of the [-C(pz)₂(2-py)] group around the methine carbon – (C3/C5) bond and results in apparent superposition of pyrazolyl/pyridyl rings. Five of the six rings were affected by the disorder. Disorder fractions for each ring were initially refined, but were subsequently fixed close to the refined values to provide a more stable refinement. The disorder fractions were constrained to the composition [(pz)₂(2-py)] at each end. The disorder of both BF₄⁻ anions was modeled using three orientations. Elongated displacement parameters for some of the F atoms indicate more orientations are probably present. Similar disorder was observed in the space group P1. Eventually all non-hydrogen atoms were refined with anisotropic displacement parameters except for the minor component of each BF₄⁻ anion (isotropic). A total of 70 restraints were used to model the disorder.

3. Results and discussion

3.1. Syntheses

The cobalt(II) chloride catalyzed Peterson rearrangement reaction between either di(pyrazolyl)carbonyl or sulfinyldi(pyrazolyl) and either aldehydes or ketones has proven to be a useful way to prepare di(pyrazolyl)alkane or other di(pyrazolyl)heteroscorpionate ligands [7a,13, 14]. The aryl(pyridyl)methanone starting materials of the form (aryl)C(O)(2-py) (left side of Fig. 1) used in this work are accessible from the corresponding aryl cyanides and '2-Lipy' as has been described elsewhere [9]. Our group has also previously reported the preparation of compounds **L1** and **L5** by using the Peterson methodology [8].

Generally, this reaction is much more difficult for diarylketones compared to either aldehydes or aliphatic ketones and this difficulty in turn is the reason for the typically low yields and long reaction times for the (aryl)C(O)(2-py) systems reported here. In the current study, it was found that the previously reported Peterson rearrangement reaction involving benzolpyridine

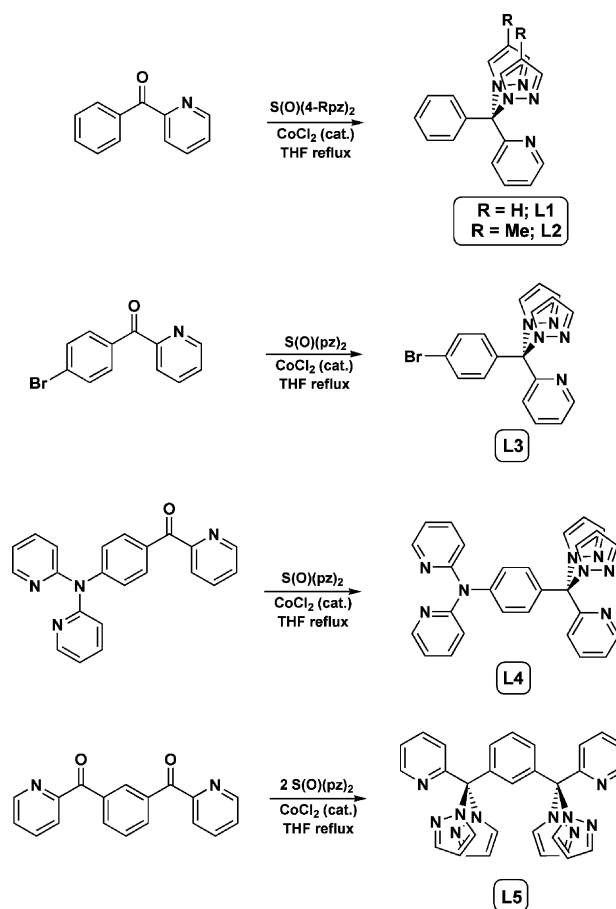


Fig. 1. Syntheses of heteroscorpionate ligands based on di(pyrazolyl)(2-pyridyl)methane units.

could be extended to 4-substituted pyrazoles as in the case of **L2**. Longer reaction times were found necessary to give yields comparable to that of unsubstituted **L1**. The use of longer chain alkyls such as in the 4-pentyl or 4-hexylpyrazolyl derivatives [15] were similarly sluggish, and difficulties that were encountered when attempting to separate the unreacted benzolpyridine and other byproducts has thus far prevented the isolation of pure compounds (owing to the similar solubilities and similar *R_f*'s on both silica and alumina). In the case of **L4**, the preparative reaction was seemingly fickle as yields were diverse and ranged from 4% to 40% independent of a constant reaction time of 3 days. Therefore, different synthetic conditions were explored in an effort to optimize the yield. Three reactions containing equal amounts (1 mmol each) of reagents *p*-(2-py)₂NC₆H₄, C(O)(2-py), S(O)(pz)₂ (prepared and isolated independently) and 10 mol% catalyst were performed simultaneously. A significant amount of product (TLC monitoring—about 30% relative spot size to the starting material) was formed when anhydrous CoCl₂ was used as a catalyst and when 3 ml of THF was used as a solvent. Only trace product (<5%) was observed when the

reaction was performed neat and no product was observed when $\text{CoCl}_2 \cdot 6\text{H}_2\text{O}$ was used as a catalyst and 3 ml of THF was present. We also explored other routes to these ligands, most notably trying to convert the phenyl pyridyl diketone to the phenyl pyridyl tetraacetal (which would then have been treated with pyrazole in the presence of acid), but the acetalization reaction proceeds very sluggishly, if at all, depending on the nature of the catalysts used (many catalysts, including indium triflate [16] and bismuth triflate [17] were explored). When it did proceed, the resulting product mixture was challenging to separate and very low yields of the tetraacetal resulted.

Tricarbonylmanganese(I) complexes of monotopic **L1–L3** ligands were prepared in high yield by the reaction between $\text{Mn}(\text{CO})_5\text{Br}$, a silver salt of a weakly coordinating anion, and then subsequent reaction with the desired heteroscorpionate, as in Fig. 2.

When similar reactions were performed with a $\text{Mn}(\text{CO})_5\text{Br}/\text{AgBF}_4$ (AgPF_6)/**L5** ligand ratio of 2:2:1, the expected homobimetallic complexes **5a** and **5b** were

obtained in good yield. However, reactions that were performed with twice the amount of ligand always produced mixtures of the homobimetallic and the desired monometallic species as indicated by elemental analyses and by the complex ^1H NMR spectrum. It has not yet been possible to separate the mixture or to otherwise obtain the pure monometallic manganese compound of **L5**. The pure solids are hygroscopic and the monometallic derivatives are soluble in polar solvents such as acetone or acetonitrile, exhibit modest solubility in CH_2Cl_2 but are only slightly soluble in chloroform and are insoluble in diethyl ether. The bimetallic compounds are considerably less soluble in acetone than their monometallic counterparts but they do show good solubility in acetonitrile and nitromethane.

The IR spectra of **1–3**, **5a** and **5b** consist of two bands centered near 2049 and 1955 cm^{-1} as expected for *fac*-carbonyls. As expected, substitution on the arene ring has no effect on the carbonyl stretching frequencies and even the 4-methyl substitution only shifts the frequencies slightly to lower energy. The room temperature NMR

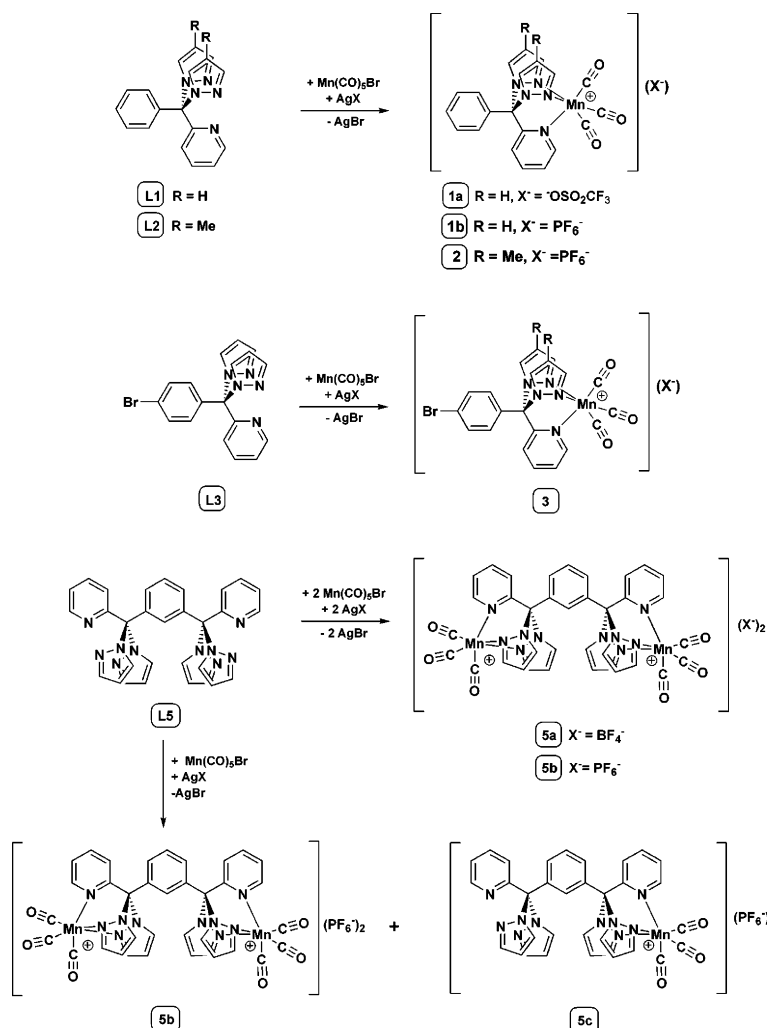


Fig. 2. Summary of reaction used to prepare tricarbonylmanganese(I) complexes of the heteroscorpionate ligands **L1–L3** and **L5**.

spectra are characterized by broad resonances and the carbonyl carbon-13 nuclei are not observed. At 55 °C, the line widths of the proton NMR resonances are greatly reduced but the resonances for the carbonyls are not observed in the ^{13}C NMR spectra. The carbonyl carbon-13 nuclei can be easily observed at temperatures of -10 °C and lower. The temperature dependence of the ^1H NMR spectra can be attributed to the restricted rotation about the aryl-methine carbon bond that is alleviated at higher temperatures as the fast exchange region is approached. This action can be envisioned as one similar to that observed for the ‘molecular turnstile’, $[(p\text{-BrC}_6\text{H}_4)_5\text{C}_5]\text{RuTp}^{4\text{Bo}}$ where $\text{Tp}^{4\text{Bo}}$ refers to hydrotris(indazolyl)borate [18]. However, in the current system restricted rotation can be envisioned to arise as a result of steric interactions involving the atoms of the arene ring and those at the 5-position of the pyrazolyl rings and at the 3-position of the pyridine ring. Presumably, the temperature dependence of the ^{13}C NMR spectra can be attributed to the restricted rotation of the arene ring (approaching the slow exchange regime) acting in combination with the reduction of the quadrupolar (^{55}Mn nucleus) component to the ^{13}C relaxation times.

3.2. Solid state structures

The structures and atom labeling schemes of the cations of **1a**, **1b**, **2**, and **5a** are provided in Fig. 3 while Table 2 summarizes important bond distances and angles.

Interestingly, the average Mn–C distances, Mn–N, and C–O bond distances are remarkably constant for the four compounds, which show that substitution along the arylC(pz)₂(2-py) ligand periphery has little effect on the electronic environment of the metal complexes. Thus, the average Mn–N bond distance is 2.04 Å for each of the four structurally characterized derivatives while the average Mn–C bond distances are 1.82, 1.83, 1.82 and 1.81 Å for **1a**, **1b**, **2**, and **5**, respectively. These values are similar to those observed in the structures of $\{[\text{HC}(3\text{-}^i\text{Prpz})_3]\text{Mn}(\text{CO})_3\}(\text{OSO}_2\text{CF}_3)$ (Mn–N 2.07, M–C 1.80 Å) [2], 1,2,4,5- $\{[(\text{OC})_3\text{Mn}(\text{pz})_3\text{CCH}_2\text{OCH}_2]_4\text{-C}_6\text{H}_2\}(\text{BF}_4)_4(\text{CH}_3\text{CN})_6(\text{Et}_2\text{O})_2$ (Mn–N 2.04, M–C 1.82 Å) [7f], $p\text{-}\{[(\text{OC})_3\text{Mn}(\text{pz})_3\text{CCH}_2\text{OCH}_2]_2\text{C}_6\text{H}_4\}$ (OSO₂CF₃)₂(THF) (Mn–N 2.04 Å, M–C 1.81 Å), and $m\text{-}\{[(\text{OC})_3\text{Mn}(\text{pz})_3\text{CCH}_2\text{OCH}_2]_2\text{C}_6\text{H}_4\}$ (BF₄)₂ (Mn–N 2.05 and 2.04 Å; M–C 1.81 Å and 1.80 Å) [7f].

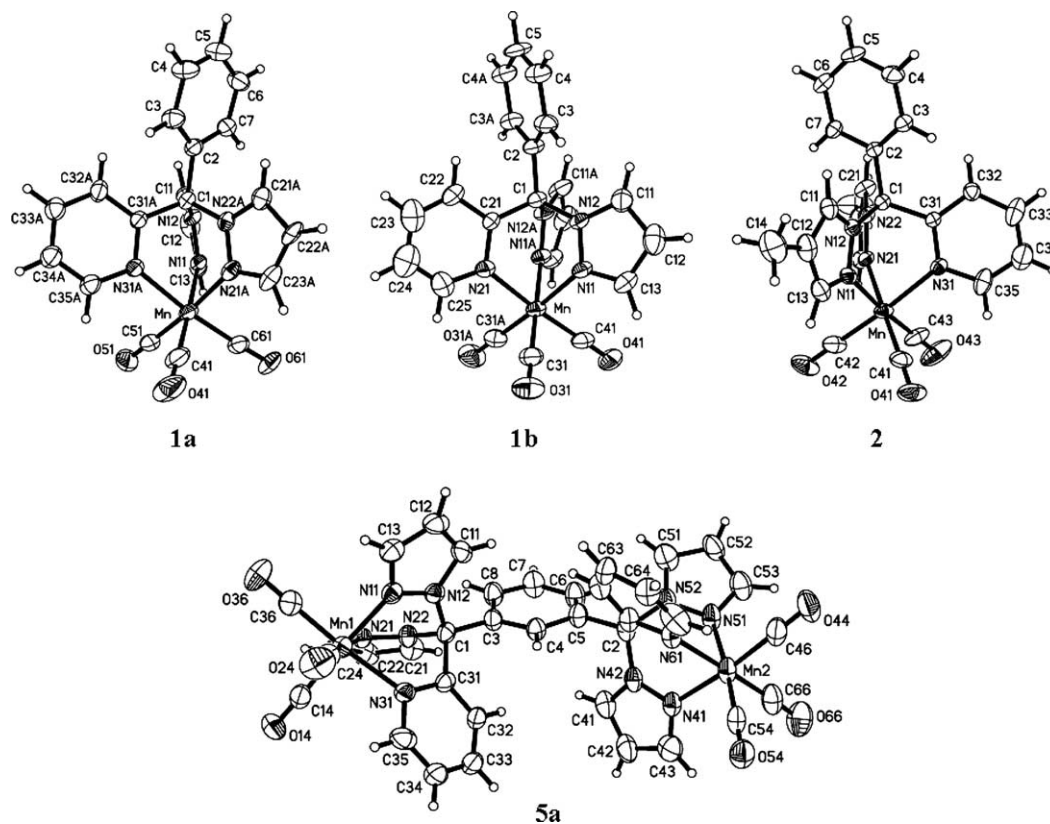


Fig. 3. ORTEP diagrams of the cations in $[\{\text{PhC}(\text{pz})_2(2\text{-py})\}\text{Mn}(\text{CO})_3](\text{O}_3\text{SCF}_3)$ (**1a**), $[\{\text{PhC}(\text{pz})_2(2\text{-py})\}\text{Mn}(\text{CO})_3](\text{PF}_6) \cdot \text{CH}_2\text{Cl}_2$ (**1b** · CH_2Cl_2), $[\{\text{PhC}(4\text{-Me})\text{pz})_2(2\text{-py})\}\text{Mn}(\text{CO})_3](\text{PF}_6)$ (**2**), and $\{m\text{-C}_6\text{H}_4[\text{C}(\text{pz})_2(2\text{-py})\text{Mn}(\text{CO})_3]_2\}(\text{BF}_4)_2 \cdot 2\text{CH}_3\text{NO}_2$ (**5a** · $2\text{CH}_3\text{NO}_2$). Only the major disorder components for **1a** and **5a** · $2\text{CH}_3\text{NO}_2$ are shown. Ellipsoids are drawn at the 50% probability level.

Table 2

Selected bond distances (Å) and angles (°) for [$\{\text{PhC}(\text{pz})_2(2\text{-py})\}\text{Mn}(\text{CO})_3\}(\text{O}_3\text{SCF}_3)$ (**1a**), [$\{\text{PhC}(\text{pz})_2(2\text{-py})\}\text{Mn}(\text{CO})_3\}(\text{PF}_6) \cdot \text{CH}_2\text{Cl}_2$ (**1b** · CH_2Cl_2), [$\{\text{PhC}(\text{C}^{4\text{-Me}}\text{pz})_2(2\text{-py})\}\text{Mn}(\text{CO})_3\}(\text{PF}_6)$ (**2**), and [$m\text{-C}_6\text{H}_4\{\text{C}(\text{pz})_2(2\text{-py})\}\text{Mn}(\text{CO})_3\}_2\}(\text{BF}_4)_2 \cdot 2\text{CH}_3\text{NO}_2$, (**5a** · $2\text{CH}_3\text{NO}_2$)

	Compound 1a	Compound 1b · CH_2Cl_2	Compound 2	Compound 5a · $2\text{CH}_3\text{NO}_2$	
<i>Bond distances</i>					
Mn–N(pz)	2.040(3)	2.054(4)	2.006(3)	1.993(2)	2.000(3)
Mn–N(pz)	2.007(3)	2.054(4)	2.036(3)	2.062(2)	2.071(3)
Mn–N(py)	2.073(3)	2.016(5)	2.089(3)	2.077(2)	2.057(2)
Mn–C	1.815(5)	1.820(5)	1.811(4)	1.804(4)	1.811(4)
Mn–C	1.821(5)	1.820(5)	1.815(4)	1.815(4)	1.817(4)
Mn–C trans py	1.818(4)	1.835(7)	1.822(4)	1.819(3)	1.807(4)
C(1)–N(pz)	1.499(4)	1.507(5)	1.486(4)	1.487(4)	1.489(4)
C(1)–N(pz)	1.506(4)	1.507(5)	1.479(4)	1.493(4)	1.499(4)
C(1)–C(py)	1.517(5)	1.514(8)	1.531(4)	1.530(4)	1.507(4)
C(1)–C(<i>ipso</i> –Ph)	1.526(5)	1.527(7)	1.534(4)	1.528(4)	1.534(4)
<i>Bond angles</i>					
N(pz)–Mn–N(pz)	85.13(12)	84.62(19)	85.71(11)	84.36(10)	83.77(10)
N(pz)–Mn–N(py)	84.47(12)	84.15(14)	83.93(10)	83.62(9)	84.87(10)
N(pz)–Mn–N(py)	82.82(12)	84.15(14)	83.07(10)	84.58(9)	83.87(10)
C–Mn–C bisect py	89.7(2)	90.8(3)	88.95(17)	89.83(14)	92.21(14)
C–Mn–C	90.80(19)	89.6(2)	89.21(16)	90.88(15)	88.67(15)
C–Mn–C	91.73(19)	89.6(2)	89.02(18)	89.99(14)	90.16(16)

3.3. Supramolecular structures

The crystal packing diagram (Fig. 4) of **1a** indicated that a layered structure is formed in the solid. A cursory examination of the supramolecular structure was undertaken in an attempt to verify this hypothesis. Since two of the three ligating rings (one pyrazolyl and the pyridyl) were disordered, the separate disorder components were examined and each gave similar results. The major pyrazolyl disorder component acts as an acceptor in a $\text{CH} \cdots \pi$ interaction with a hydrogen from a well-behaved phenyl ring $\{\text{CH}(6)\text{-ring centroid (Ct)}[\text{N}(21a)] = 2.85 \text{ \AA}$, C-H-Ct angle = $140.5^\circ\}$. This interaction results in the formation of dimers of cations (three of these dimers are shown

in the left of Fig. 5). Three sets of $\text{CH} \cdots \text{O}$ interactions result in chains that run along the $[1\ 1\ 1]$ direction. One involves a hydrogen at the 5-position of the well-ordered pyrazolyl ring and the oxygen of a triflate counteranion $[\text{CH}(11)\text{-O}(3) 2.29 \text{ \AA}$, $145.4^\circ]$ while the other two involve hydrogens of the disordered pyrazolyl/pyridyl ring systems $[\text{CH}(22a)\text{-O}(2) 2.31 \text{ \AA}$, 173.1° ; $\text{CH}(34a)\text{-O}(2) 2.30 \text{ \AA}$, $135.4^\circ]$. The integrity of the chain remains when the minor disorder component is examined. The chains are held together along the a directions into sheets by longer $\text{CH} \cdots \text{O}$ interactions between $\text{CH}(23a)$ and $\text{O}(2)$ (2.55 \AA , 157.3°).

The exquisite three-dimensional supramolecular structure of **1b** (Fig. 6) is organized solely by $\text{CH} \cdots \text{F}$

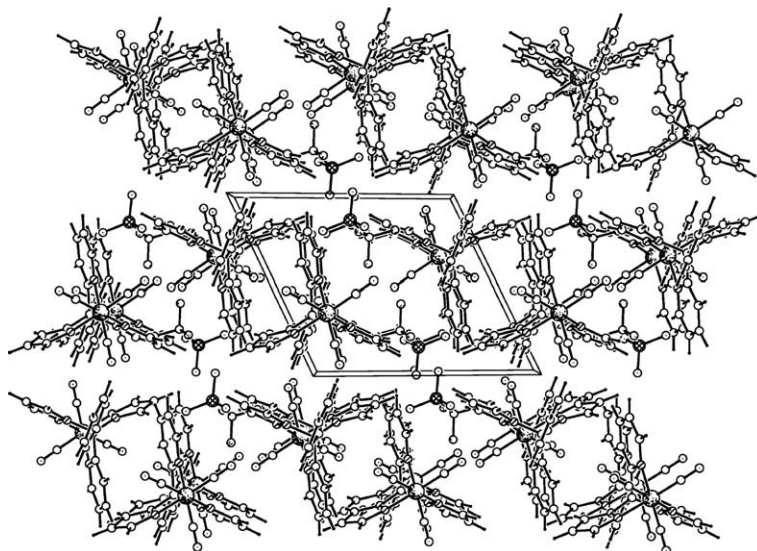


Fig. 4. Crystal packing diagram of **1a** emphasizing layered structure of the compound.

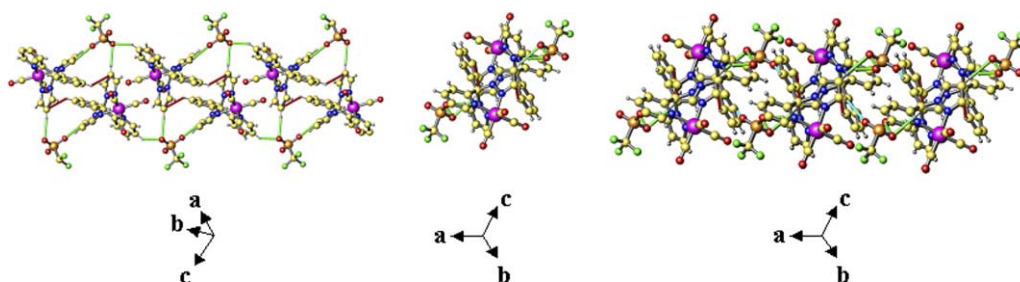


Fig. 5. Supramolecular sheet structure of the major disorder component of **1a**. *Left*: chains held together via CH- π (red lines, left) and CH-O interactions (green lines, left and blue lines, right). *Middle*: end on view of chain. *Right*: Stacking of chains along the *a* directions as a result of CH-O interactions (blue lines).

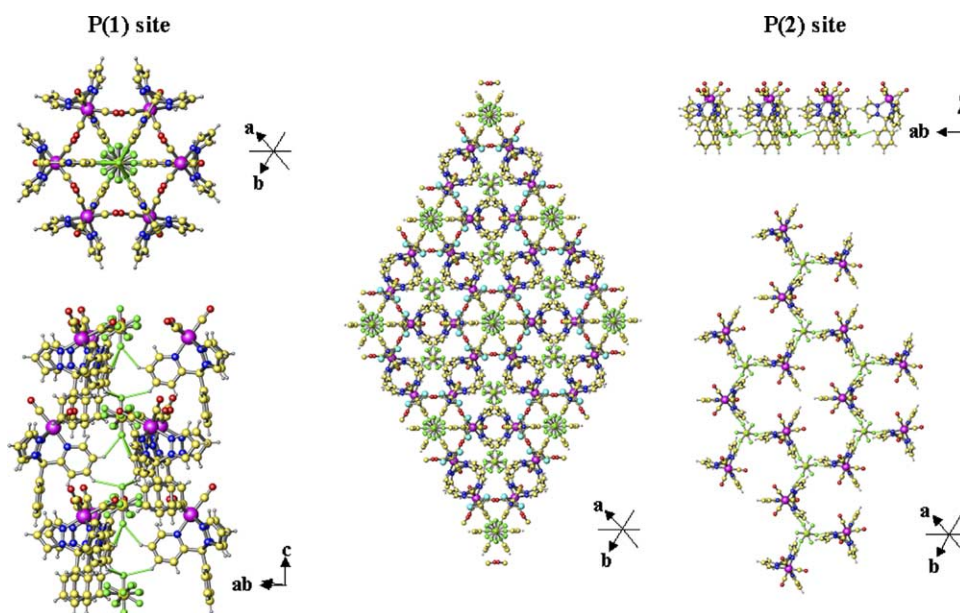


Fig. 6. Supramolecular Structure of $\{[\text{PhC}(\text{pz}_2)(2\text{-py})\}\text{Mn}(\text{CO})_3(\text{PF}_6) \cdot \text{CH}_2\text{Cl}_2$ (**1b** \cdot CH_2Cl_2). *Left*: Hexagonal tube of cations held together by trifurcated CH \cdots F interactions (green lines) with well-behaved fluorines on disordered PF_6^- anions and three pyridyl ring hydrogens. *Center*: Crystal packing with CH_2Cl_2 molecules (light blue spheres). *Right*: Top view of two sheets PF_6^- organize the cations into a sheet in the *ab* plane.

interactions that are shorter than the 2.6 Å cutoff proposed to be indicative of weak hydrogen bonding [3c]. There are two independent PF_6^- sites in the lattice and each affords connectivity in a different manner. The first site containing P(1) is rotationally disordered about the F(11)–P(1)–F(15) axis. The well-ordered fluorines F(11) and F(15) each participate in trifurcated CH \cdots F interactions with hydrogen atoms at the *p*- and *m*-positions, respectively, of the pyridyl ring on the cations (Fig. 6, left) [CH(24)–F(11) 2.37 Å, 137°; CH(23)–F(15) 2.46 Å, 139°].

This arrangement creates a hexagonal tube of cations filled with an array of anions directed along *c*. The tubes are connected in the *ab* plane as a result of CH \cdots F interactions involving the *o*-hydrogen of the phenyl ring H(3) and F(22) of the second independent PF_6^- anion as in Fig. 6 (right) [CH(3)–F(22) 2.48 Å, 113°]. This structure is further supported by other short (<2.6 Å) CH–F interactions (not shown).

The chiral three-dimensional supramolecular structure of **2** is organized by CH \cdots π , CH \cdots O, and CH \cdots F interactions (Table 3). The result of the CH \cdots π and CH \cdots O interactions is stacked sheets of left-handed helices where each adjacent sheet is related by the 2_1 screw axis (Fig. 7). Thus, each sheet is held together by a set of CH \cdots π interactions between C(5)H(5) of

Table 3
Summary of short CH \cdots F interactions in the structure of $[\text{PhC}(\text{pz}^{4\text{Me}})_2(2\text{-py})\text{Mn}(\text{CO})_3(\text{PF}_6)_2]$

Donor \cdots acceptor	H \cdots F (Å)	C(H) \cdots F (°)
C(7)H(7) \cdots F(2)	2.50	134.1
C(13)H(13) \cdots F(2)	2.44	154.0
C(23)H(23) \cdots F(3)	2.47	133.1
C(24)H(24b) \cdots F(3)	2.54	120.6
C(32)H(32) \cdots F(1)	2.53	119.3
C(34)H(34) \cdots F(4)	2.49	144.3
C(35)H(35) \cdots F(6)	2.29	146.1

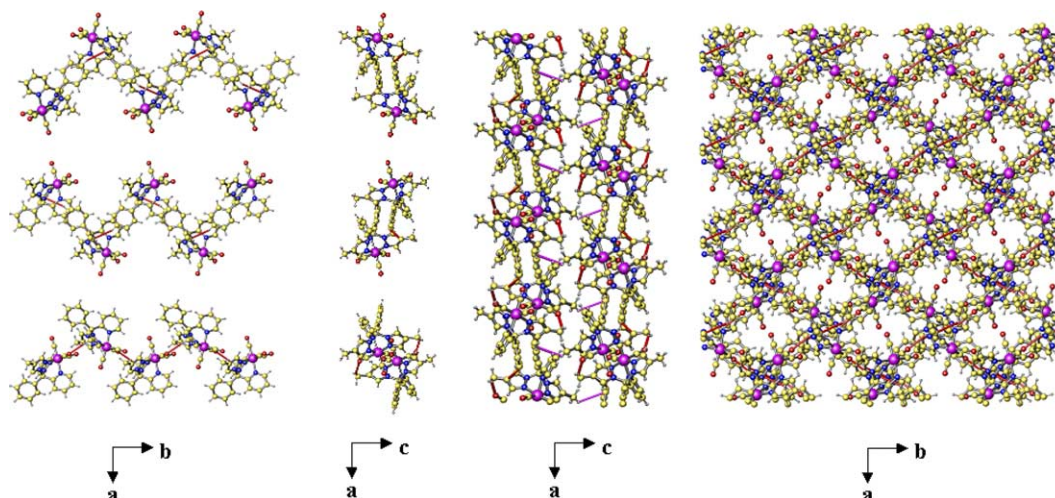


Fig. 7. Supramolecular framework of **2** composed of only $\text{CH}\cdots\pi$ and $\text{CH}\cdots\text{O}$ interactions (red lines). *Top left*: Left-handed helix comprised of $\text{CH}\cdots\pi$ interactions. *Middle left*: Left-handed helix comprised of $\text{CH}\cdots\text{O}$ interactions. The combination of this $\text{CH}\cdots\text{O}$ interaction with either of the $\text{CH}\cdots\pi$ interactions above creates sheets in the ab plane. *Middle*: Stacking of two sheets of left- and right-handed helices by $\text{CH}\cdots\pi$ interactions (pink lines). *Right*: View onto top of two sheets. PF_6^- anions reside in channels created by stacking of sheets.

the phenyl ring acting as a hydrogen donor and the centroid (Ct) of the pyrazolyl ring containing N(11) with C(5)H(5)–Ct[N(11)] 2.74 Å, 162.3° and by a set of $\text{CH}\cdots\text{O}$ interactions involving a 4-methyl hydrogen C(14)H(14c) and the carbonyl oxygen O(43) [C(14)H(14c)–O(43), 2.56 Å, 153.0°]. The sheets are held together by another $\text{CH}\cdots\pi$ interaction that occurs between a methyl pyrazolyl hydrogen donor and the phenyl ring that acts as an acceptor with C(24)H(24b)–Ct[Ph] of 3.20 Å and 102°. These interactions form a porous network of cations as in Fig. 7, right. The PF_6^- anions reside in the channels and support the network of cations in all three dimensions by numerous $\text{CH}\cdots\text{F}$ interactions that are shorter than the 2.6 Å cutoff proposed to be indicative of weak hydrogen bonding [3c]. Extensive disorder of the ligand and tetrafluoroborate anions in **5a** prevented a comprehensive examination of its supramolecular structure. An inspection of the packing arrangement reveals that the cationic building blocks are arranged into chains along the body diagonal of the unit cell by intercationic contacts between the π clouds of the carbonyl groups bonded to manganese atoms.

4. Conclusions

We have shown that the Peterson rearrangement reaction between either di(pyrazolyl)carbonyl or sulfinyldi(pyrazolyl) and appropriately substituted ketones is a useful methodology to prepared ligands containing the $[\text{C}(\text{pz})_2(2\text{-py})]$ -scorpionate moiety. The $\text{Mn}(\text{CO})_3$ complexes of these ligands show interesting structural diversity, with the complexes being organized in the so-

lid state by a complex array of non-covalent forces. Particularly interesting is the three dimensional structure of $\{[\kappa^3\text{-PhC}(\text{pz})_2(2\text{-py})]\text{Mn}(\text{CO})_3\}(\text{PF}_6)$, organized exclusively by $\text{CH}\cdots\text{F}$ interactions. In all these complexes, the $[\text{C}(\text{pz})_2(2\text{-py})]$ -scorpionate unit shows κ^3 -coordination, as opposed to the κ^2 -coordination observed in silver(I) chemistry. We have prepared the first bimetallic complex of this ligand type, $[(\text{CO})_3\text{Mn}\{\mu\text{-}m\text{-C}_6\text{H}_4[\text{C}(\text{pz})_2(2\text{-py})]_2\}\text{Mn}(\text{CO})_3](\text{BF}_4)_2$. Unfortunately, we have been unable to prepare the monometallic analog, $\{m\text{-C}_6\text{H}_4[\text{C}(\text{pz})_2(2\text{-py})]_2\}\text{Mn}(\text{CO})_3(\text{BF}_4)$, for use in the syntheses of heterobimetallic complexes. Clearly, these ligands and their derivatives are applicable to the chemistry of many other metal systems.

5. Supplementary material

Crystallographic data for the structural analysis has been deposited with the Cambridge crystallographic Centre, CCDC 247499-247502. Copies of this information may be obtained free of charge from the director, CCDC, 12 Union Road, Cambridge, CB2 1EZ UK (fax +44-1223-336-033; e-mail deposit@ccdc.cam.ac.uk, or www: <http://www.ccdc.cam.ac.uk>).

Acknowledgement

We thank the National Science Foundation (CHE-0414239) for support. The Bruker CCD Single Crystal Diffractometer was purchased using funds provided by the NSF Instrumentation for Materials Research Program through Grant DMR:9975623.

References

- [1] (a) O.R. Evans, W. Lin, *Acc. Chem. Res.* 35 (2002) 511;
(b) D. Braga, *J. Chem. Soc., Dalton Trans.* 21 (2000) 3705;
(c) S.J. Lee, A. Hu, W. Lin, *J. Am. Chem. Soc.* 124 (2002) 12948.
- [2] D.L. Reger, T.C. Grattan, K.J. Brown, C.A. Little, J.J.S. Lamba, A.L. Rheingold, R.D. Sommer, *J. Organomet. Chem.* 607 (2000) 120.
- [3] (a) Weak hydrogen bonds (X–H...Y) involve less electronegative atoms; we discuss here only those of the C–H...Y type (Y = O, F). See for example: M.J. Calhorda, *Chem. Commun.* (2000) 801;
(b) G.R. Desiraju, *Acc. Chem. Res.* 29 (1996) 441;
(c) F. Grepioni, G. Cozzani, S.M. Draper, N. Scully, D. Braga, *Organometallics* 17 (1998) 296;
(d) H.C. Weiss, R. Boese, H.L. Smith, M.M. Haley, *Chem. Commun.* (1997) 2403.
- [4] C.J. Janiak, *J. Chem. Soc., Dalton Trans.* (2000) 3885, and references therein.
- [5] (a) H. Takahashi, S. Tsuboyama, Y. Umezawa, K. Honda, M. Nishio, *Tetrahedron* 56 (2000) 6185;
(b) S. Tsuzuki, K. Honda, T. Uchimaru, M. Mikami, K. Tanabe, *J. Am. Chem. Soc.* 122 (2000) 11450;
(c) O. Seneque, M. Giorgi, O. Reinaud, *Chem. Commun.* (2001) 984;
(d) H.C. Weiss, D. Blaser, R. Boese, B.M. Doughan, M.M. Haley, *Chem. Commun.* (1997) 1703;
(e) N.N.L. Madhavi, A.K. Katz, H.L. Carrell, A. Nangia, G.R. Desiraju, *Chem. Commun.* (1997) 2249;
(f) N.N.L. Madhavi, A.K. Katz, H.L. Carrell, A. Nangia, G.R. Desiraju, *Chem. Commun.* (1997) 1953.
- [6] (a) D.S. Reddy, D.C. Craig, G.R. Desiraju, *J. Am. Chem. Soc.* 118 (1996) 4090;
(b) J. Kowalik, D. VanDerveer, C. Clower, L.M. Tolbert, *Chem. Commun.* (1999) 2007;
(c) M. Freytag, P.G. Jones, B. Ahrens, A.K. Fischer, *New J. Chem.* 23 (1999) 1137;
(d) R. Thaimattam, D.S. Reddy, F. Xue, T.C.W. Mak, A. Nangia, G.R. Desiraju, *New J. Chem.* (1998) 143.
- [7] (a) D.L. Reger, K.J. Brown, J.R. Gardinier, M.D. Smith, *Organometallics* 22 (2003) 4973;
(b) D.L. Reger, J.R. Gardinier, R.F. Semeniuc, M.D. Smith, *J. Chem. Soc., Dalton Trans.* (2003) 1712;
(c) D.L. Reger, T.D. Wright, R.F. Semeniuc, T.C. Grattan, M.D. Smith, *Inorg. Chem.* 40 (2001) 6212;
(d) D.L. Reger, R.F. Semeniuc, M.D. Smith, *Eur J. Inorg. Chem.* (2002) 543;
(e) D.L. Reger, R.F. Semeniuc, M.D. Smith, *J. Chem. Soc. Dalton Trans.* (2002) 476;
(f) D.L. Reger, R.F. Semeniuc, M.D. Smith, *J. Organomet. Chem.* 666 (2003) 87;
(g) D.L. Reger, R.F. Semeniuc, I. Sillaghi-Dumitrescu, M.D. Smith, *Inorg. Chem.* 42 (2003) 3751;
(h) D.L. Reger, R.F. Semeniuc, V. Rassolov, M.D. Smith, *Inorg. Chem.* 43 (2004) 537.
- [8] D.L. Reger, J.R. Gardinier, M.D. Smith, *Polyhedron* 23 (2004) 291.
- [9] D.L. Reger, J.R. Gardinier, M.D. Smith, P.J. Pellechia, *Inorg. Chem.* 42 (2003) 482.
- [10] D.L. Reger, J.R. Gardinier, M.D. Smith, *Inorg. Chim. Acta* 352 (2003) 151.
- [11] SMART Version 5.625, SAINT+ Version 6.02a and SADABS. Bruker Analytical X-ray Systems, Inc., Madison, WI, USA, 1998.
- [12] G.M. Sheldrick, SHELXTL, Version 5.1, Bruker Analytical X-ray Systems, Inc, Madison, WI, USA, 1997.
- [13] D.L. Reger, R.P. Watson, J.R. Gardinier, M.D. Smith, *Inorg. Chem.* 43 (2004) 6609.
- [14] K.I. Thé, L.K. Peterson, *Can. J. Chem.* 51 (1973) 422.
- [15] D.L. Reger, J.R. Gardinier, T.C. Grattan, M.R. Smith, M.D. Smith, *New J. Chem.* (2003) 1670.
- [16] S. Muthusamy, S.A. Babu, C. Gunanathan, *Tetrahedron* 58 (2002) 7897.
- [17] N.M. Leonard, M.C. Oswald, D.A. Freiberg, B.A. Nattier, R.C. Smith, R.S. Mohan, *J. Org. Chem.* 67 (2002) 5202.
- [18] A. Carella, J. Jaud, G. Rapenne, J.-P. Launey, *Chem. Commun.* 19 (2003) 2434.